Diffuse x-ray scattering from thermal donors in Czochralski-grown silicon

T. Yamazaki and I. Hashimoto

Department of Physics, Science University of Tokyo, 1-3 Kagurazaka, Shinjuku-ku, Tokyo 162, Japan

The diffuse x-ray (Cu $K\alpha_1$) scattering from Czochralski-grown (Cz) silicon crystals after annealing at 450 °C for 24 h has been investigated. The x-ray measurements have been made near the (400) and ($3\bar{1}1$) Bragg reflections in directions parallel and perpendicular to the scattering vector. All the characteristic features have been predicted by the theory for scattering from defect clusters with weak displacement fields (Huang scattering). It is shown that the long-range part of their displacement fields has an orthorhombic symmetry and the defects are the interstitial type. Furthermore, by comparing the symmetry of the diffuse scattering intensities with that of displacement fields around the thermal donor models in Cz Si, it is found that an NL8 or IO_2 (self-interstitial and two oxygens) model is reasonable as a core structure of thermal donors. [S0163-1829(97)00221-X]

I. INTRODUCTION

Diffuse x-ray scattering has been used for 40 years as a very powerful method for the investigation of point defects and their clusters.[1-9] Diffuse scattering is suitable for the measurement of the symmetry and strength of defects and is also a very sensitive method for observing the clustering of point defects during annealing. Since most theoretical model calculations pertain to the noble metals such as Cu and Ni, it has been preferred[2,4,6] to do the diffuse x-ray scattering measurements also on these metals. For semiconductors, however, comparison between the scattering results and the theoretical calculations has been limited to larger defects, especially dislocation loops,[8,9] and has never been applied to small defects like thermal donor (TD) complexes.

TD complexes arising after heat treatments at around 450 °C in oxygen-rich Czochralski-grown (Cz) silicon have been studied in detail since their discovery.[10] Much important experimental information of the properties has been obtained and many structural models have been proposed.[11] However, no conclusive information to determine the TD structure has been obtained yet. In order to determine the structure of the oxygen-related TD defects, it is helpful to give a short summary of the characteristic features of much of the experimental information[11-13] available.

(1) There is a series of TD_n complexes,[14-18] usually $n=1-9$; recently up to 17 have been identified,[12,19] produced by a clustering of oxygen atoms during annealing in the temperature range of 300–550 °C and dissociated by annealing at temperatures higher than 550 °C. Each species of TD_n sequentially appears with increasing the annealing time. An initial rate of TD formation is proportional to the fourth power[20] of the initial oxygen concentration, and the total TD concentration A approaches its maximum value according to the law of $\ln[A_{\max}-A(t)/A_{\max}]=-kt$, where t is the annealing time.[21] The maximum of the total TD concentration is approximately proportional to the cube of the initial oxygen concentration[14,21] and TD_3 and TD_4 have attained the highest maximum concentrations in the nine species after annealing for about 24 h at 450 °C.[22]

(2) TD is a double donor[14-16,18,23] and the energy levels are distributed at around $E_c-0.07$ and 0.15 eV,[12] forming a succession of increasingly shallow states. The electron paramagnetic resonance (EPR) center[24] NL8 correlates with these characteristic electronic transitions.[25-27]

(3) The dominant TD species after annealing for over 10 h at 450 °C have a C_{2v} point-group symmetry[25,28] (C_2 rotation axis [001] and mirror planes, two in each of the perpendicular {110} planes). In the cluster of TD_n series the anisotropy increases with n.[29] Therefore, it is generally supposed that all TD's have a common core[12,13] and that TD_{n+1} is generated from TD_n by the addition of one extra oxygen atom[21] in a (110) plane.

Based on accumulating knowledge about TD complexes, a large number of core structure models have been proposed. According to Deák *et al.*,[30] they can be classified into four groups.

(a) Oxygen-only complexes: (O_Y) configuration, one oxygen is bonded to three silicon atoms to form the threefold coodinate, what is called a *y*-lid; $(O_i)_2$,[31] O_i occupies a puckered bond-center position between two neighboring silicon atoms;[32,33] $(O_r)_2$, the four-member ring structure in which two threefold-coordinated oxygens and two silicons;[30,31] $(O_Y)_2$;[34,35] interstitial O_2 molecule,[36] two oxygens intercepting parallel Si-Si bonds in a (111) plane and also bonded to each other; and two O_3 complexes,[37] one is (O_Y) stabilized by O_i atoms on both sides, the other is that two oxygen atoms intervene at the nearby bond-centered sites, and the silicon atom bonded both sides with these two oxygens is repelled upward and the broken two bonds with other silicon atoms repaired by addition of one more oxygen atom.

(b) Oxygen + vacancy complexes: VO, one vacancy and one O_i;[38,39] VO_2, one vacancy and two O_i's;[36,40] and VO_4, one vacancy and two bond-centered O_2 molecules.[36,41]

(c) Oxygen + semivacancy complexes: The Ourmazd-Bourret-Schröter (OBS) model[22] and NL8 center[41] proposed by the electron-nuclear double resonance (ENDOR) investigations.

(d) Oxygen + self-interstitial complex: IO_2, one self-interstitial and two threefold coordinated oxygens.[13,42]

The purpose of this paper is to propose experimental data

to determine the TD's core structure by comparing the distribution of diffuse x-ray intensity from the TD complexes with that theoretically calculated from the above complicated TD core models. The following section gives a short summary of the theoretical background of diffuse x-ray scattering. Section III contains the experimental procedures. The results of the diffuse scattering measurements are discussed in Sec. IV.

II. THEORETICAL BACKGROUND

The most important features of the theory of diffuse x-ray scattering for understanding the Si results are summarized here. For further details and a complete review of the literature we refer to Dederichs,[43] the papers of Trinkaus,[44] Ehrhart et al.,[1-3] and Morozov and Bublik.[8]

Assuming a statistical distribution of defects, low defect densities, and a linear superposition of the displacement fields around the defects, one obtains, for the diffuse scattering cross section per atom close to the Bragg peaks,

$$S_{\text{diff}}(\boldsymbol{k}) = S_{\text{Huang}}(\boldsymbol{k}) + S_{\text{anti}}(\boldsymbol{k}). \qquad (1)$$

The main term is the Huang scattering

$$S_{\text{Huang}}(\boldsymbol{k}) = c f_{\boldsymbol{h}}^2 |\boldsymbol{h} \cdot \boldsymbol{t}(\boldsymbol{q})|^2, \qquad (2)$$

where c is the concentration of defects, $f_{\boldsymbol{h}}$ the atomic scattering factor, $\boldsymbol{k}$ the scattering vector, $\boldsymbol{h}$ the nearest reciprocal lattice vector, $\boldsymbol{q} = \boldsymbol{k} - \boldsymbol{h}$, and $\boldsymbol{t}(\boldsymbol{q})$ the Fourier transform of the displacement field of one defect (single-defect approximation). For the case of small values of $\boldsymbol{q}$, $\boldsymbol{t}(\boldsymbol{q})$ can be evaluated by elastic continuum theory. In this approximation, the symmetry and strength of the long-range part of the displacement field are determined by the dipole force tensor P_{ij} and the radial variation is like $1/R^2$, where R is the distance from the defect center. Expressing $\boldsymbol{t}(\boldsymbol{q})$ in terms of the components of the dipole force tensor P_{ij}, we get for cubic crystals

$$S_{\text{Huang}}(\boldsymbol{q}) = c f_{\boldsymbol{h}}^2 \left(\frac{\boldsymbol{h}}{\boldsymbol{q}}\right)^2 \frac{1}{V_c^2} [\gamma^{(1)} \pi^{(1)} + \gamma^{(2)} \pi^{(2)} + \gamma^{(3)} \pi^{(3)}], \qquad (3)$$

where $\gamma^{(1)}$, $\gamma^{(2)}$, and $\gamma^{(3)}$ are factors which depend on the elastic constants of the medium and on the directions of $\boldsymbol{q}$ and $\boldsymbol{h}$. V_c is the atomic volume, and $\pi^{(1)}$, $\pi^{(2)}$, and $\pi^{(3)}$ are quadratic expressions of the dipole force tensor components:

$$\pi^{(1)} = \frac{1}{3}\left(\sum_i P_{ii}\right)^2 = \frac{1}{3} P^2, \qquad (4a)$$

$$\pi^{(2)} = \frac{1}{6}\sum_{i>j} (P_{ii} - P_{jj})^2, \qquad (4b)$$

$$\pi^{(3)} = \frac{2}{3}\sum_{i>j} P_{ij}^2. \qquad (4c)$$

The quantity $P = \text{Tr } P_{ij} = (3\pi^{(1)})^{1/2}$ characterizes the strength of the defect. It also determines the lattice parameter change as

$$\frac{\Delta a}{a} = \frac{1}{3}\frac{\Delta V}{V} = c \frac{P}{3V_c(c_{11} + 2c_{12})}, \qquad (5)$$

TABLE I. Parameters $\gamma^{(1)}$, $\gamma^{(2)}$, and $\gamma^{(3)}$ entering into Eq. (3) for two reflections and q directions used in the present investigation. The parameters have been calculated according to the formulas given in Refs. 43 and 44 using the room-temperature elastic constants of Si (Ref. 54): $c_{11} = 1.6564 \times 10^{12}$ dyn/cm^2. The parameters $\gamma^{(i)}$ are given in units of $1/3c_{11}^2 = 1.215 \times 10^{-25}$ dyn^{-2} cm^4.

Type of reflection	Direction of $\boldsymbol{q}$	$\gamma^{(1)}$	$\gamma^{(2)}$	$\gamma^{(3)}$
$(h00)$	[100]	1	2	0
	[011]	0	0	8.22
$(3\bar{1}1)$	[011]	0	2.89	1.23

where c_{11} and c_{12} are elastic constants. Therefore, the measurements of both S_{Huang} and of $\Delta a/a$ can determine the absolute value of the defect density c. The quantities $\pi^{(2)}$ and $\pi^{(3)}$ characterize the deviation from the cubic symmetry of the long-range displacement field.

The shape of the diffuse x-ray scattering intensity distribution around the different reflections is determined by the variation of the coefficients $\gamma^{(1)} - \gamma^{(3)}$ in the square brackets of Eq. (3) with the directions of $\boldsymbol{q}$ and $\boldsymbol{h}$ and by the magnitudes of the defect parameters $\pi^{(1)} - \pi^{(3)}$. For Si, the factors $\gamma^{(1)} - \gamma^{(3)}$ in Eq. (3) are summarized for different directions and reflections in Table I. Inspection of this table reveals that by combining the measuring direction a unique discrimination between cubic ($\pi^{(2)} = \pi^{(3)} = 0$), tetragonal ($\pi^{(2)} > 0$, $\pi^{(3)} = 0$), trigonal ($\pi^{(2)} = 0$, $\pi^{(3)} > 0$), and orthorhombic ($\pi^{(2)}$, $\pi^{(3)} > 0$) symmetry of the long-range displacement field of the defects is possible.

The antisymmetric contribution S_{anti} to the diffuse scattering intensity in Eq. (1) is given by

$$S_{\text{anti}} = 2 c f_{\boldsymbol{k}}^2 \eta \frac{\boldsymbol{h}}{\boldsymbol{q}} \frac{1}{V_c} \left(\frac{1}{3}\gamma^{(1)}\right)^{1/2} P, \qquad (6)$$

with

$$\eta = \sum_n (1 - \cos\boldsymbol{h}\cdot\boldsymbol{t}^n) - \text{Re}\frac{f_{\boldsymbol{h}}^D}{f_{\boldsymbol{h}}}, \qquad (7)$$

where $f_{\boldsymbol{h}}^D$ is the scattering factor of the defect and $\boldsymbol{t}^n$ the static displacement of the atom n due to the defect. Equation (6) holds for defects whose long-range displacement fields have cubic symmetry.[1]

$S_{\text{anti}}(\boldsymbol{k})$ is antisymmetric with respect to the direction of $\boldsymbol{q}$; therefore it can easily be separated from the symmetric $S_{\text{Huang}}(\boldsymbol{k})$ by averaging the experimentally observed intensities S_{diff} at equal distances but opposite directions from the Bragg peak. For defects with large local displacements, like single interstitials, interstitial clusters, dislocation loops, etc., the first term of Eq. (7) usually outweighs the contribution to η from the scattering amplitude $f_{\boldsymbol{h}}^D$ of the defect itself. For such defects η is always positive, so that the sign of long-range displacements can be determined directly from the sign of S_{anti}.

When the point defects are clustering, the diffuse scattering comes from the strongly distorted region around the defects. The diffuse scattering for larger values of $q \gtrsim 1/R_0$ can
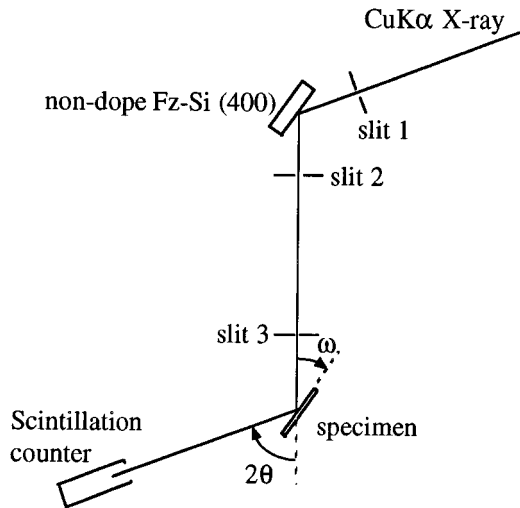
FIG. 1. Schematic view of the measuring system.

be described by a Stokes-Wilson approximation,[44] which shows the characteristic proportionality to q^{-4} in contrast to S_{Huang}.

The main principles of double-crystal measurements and the analysis of the diffuse x-ray intensity distribution can be found in the above paragraphs. However, a more correct analysis of the diffuse x-ray intensity has been carried out by Krivoglaz.[45] It becomes possible to obtain more precise information on defect sizes and their types.

For the case of widely opened detector slits, the x-ray detector measures scattered intensities around every $q = (q_0^2 + q_1^2)^{1/2}$, where the vector q_1 which satisfies the inequality $0 < q_1 < \infty$ belongs to the tangent plane including the point $q_0 = \Delta \theta h \cos \theta$. The q_0 determines the minimum distance between the reciprocal lattice site and the Ewald sphere with the angular deviation $\Delta \theta$ from the Bragg position.

The integral x-ray intensity and its dependence on q_0 are determined by the integral

$$\int_0^\infty \frac{q_d^{m-2} q_1 dq_1}{(q_1^2 + q_0^2)^{m/2}}. \tag{8}$$

Here m is the power factor in the power law expression $I(q) \propto q^{-m}$, and for clusters the vector q_d is determined by the expression $q_d = R_0^{-1}$ for different q_0. Then the integration of Eq. (8) gives as

$$I(q_0) \propto \begin{cases} \ln[q_d \exp(0.5)/q_0] & \text{for } q_0 < q_d, \\ q_d^2/2q_0^2 & \text{for } q_0 > q_d. \end{cases} \tag{9}$$

III. EXPERIMENTAL PROCEDURES

A. X-ray setups

The diffuse x-ray scattering measurements were performed at room temperature in the so-called integral geometry (widely opened counter slits). The double-crystal diffractometer system (Rigaku Denki SLX-1) schematically shown in Fig. 1 with an 18 kW rotating anode x-ray source and Cu $K\alpha$ radiation was used. It was composed of a vacuum path which led the x-ray to the monochromator, a

0.5 mm slit (slit 1) in front of the monochromator, the monochromator crystal which selected the $K\alpha_1$ radiation by a (100)-cut nondoped Fz Si single crystal for the symmetrical incidence (400) reflection, a 0.5 mm slit (slit 2), a 0.2 mm slit (slit 3), the sample holding at the high-precision three-axis goniometer, and the scintillation counter (the energy resolution $\Delta E/E \simeq 40\%$). The incident x-ray beam area onto the specimen surface was 0.2×5 mm^2. The range of angular deviation of the second crystal from the accurate Bragg position was $\pm 2°$ and the angular scanning step was $0.05°$. In order to obtain an accurate Bragg peak, the scanning was carried out using a step of $1''$.

In our systems, the background was less than 10 counts/min. According to Klug and Alexander,[46] if N_T is the total number of counts recorded in time t and N_B is that of background counts in the same time, the probable error u_p is given by

$$u_p = \frac{1.64}{R-1} \left[\frac{R(R+1)}{N_T} \right]^{1/2} \tag{10}$$

for a 90% confidence level (here, $R = N_T/N_B$). For $u_p = 3\%$, this reduces to

$$N_T = 3000 \frac{R(R+1)}{(R-1)^2}. \tag{11}$$

Assuming a signal-to-background ratio of 30, N_T is of the order of 3×10^3. Taking into account this criterion, counts in each step are accumulated in the scaler for 2000–4000 s.

The scattering intensity around the reciprocal lattice point h was measured in a direction parallel to h by rotating the sample and the counter at the ratio of 1:2. It was also measured in a direction perpendicular to h by rotating the sample with the counter angle fixed at $2\theta_B$ (θ_B is the Bragg angle). The diffuse x-ray scattering intensity was obtained by subtracting the intensity of the nondoped Fz Si single crystal from the total intensity. In this time, thermal diffuse scattering and other background scattering were automatically removed.

B. Correction of intensities to absolute units

The absolute diffuse scattering cross sections S [given in electron units (e.u.)] were obtained from the known cross section of a polystyrene (C_8H_8) reference sample by comparison of the scattered intensities.[47] The polarization factor p depends on the scattering angle of the monochromator and that of the sample and was calculated for "mosaic crystals." For thin crystals and for asymmetrical geometry, corrections are necessary for scattered intensities I. The correction factors $k = I_{\text{ideal}}/I_{\text{actual}}$ were calculated according to the International Tables[48] and are collected in Table II.

In order to determine the absolute scattering cross section S, the square of the atomic structure factor, $f_h^2 = (f + \Delta f')^2$, must be known for the evaluation of $\pi^{(1)} - \pi^{(3)}$ from Eq. (3). f_h^2 is reduced by the thermal Debye-Waller Factor (DWF) neglected in Eq. (3). According to the International Tables, the values of f_h were taken and the DWF was calculated for the temperature of 293 K. The thermal Debye pa-

TABLE II. Parameters used for conversion to absolute intensities.

Reflection	Geometry, θ_B (300 K)	p	Absorption correction k	DWF (293 K)	$(f_0 + \Delta f')^2$
(400)	Symmetrical reflection 34.57	0.902	1.000	0.908	59.55
$(3\bar{1}\bar{1})$	Asymmetrical reflection 28.06	0.922	8.647	0.935	69.96

rameters were taken as average values of $\Theta_D = 505$ and 658 K. All values are collected in Table II.

C. Samples

A precisely chemically polished (100) surface cut from the nondoped Fz Si single crystal was used as the reference specimen. The sample being investigated was a p-type Cz Si wafer which was doped with B having a 600 μm thick and a (100) surface orientation. The resistivity was in the range of 4–6 Ω cm, and it initially contained interstitial oxygen of 1.7×10^{18} cm^{-3} and substitutinal carbon of 1.0×10^{17} cm^{-3}. The samples were cut from the wafer to sizes of about 5 $\times 15$ mm^2, preannealed for 5 min over 750 °C, and annealed for 24 h at 450 °C in a vacuum furnace ($\sim 1 \times 10^{-6}$ Torr). Before the x-ray measurements, the samples were chemically etched by an acid mixture (CH$_3$COOH:HNO$_3$:HF=10:4:1) to remove the low-defect-density region of about 20 μm at the front surface. After the above heat treatments, the concentrations of interstitial oxygen atoms and substitutional carbon atoms were estimated from the 9 μm and the 16.5 μm absorption bands obtained at room temperature by using a Fourier transform infra-red (FTIR) spectrometer using the conversion factors of 2.45×10^{17} cm^{-2} (ASTM F121-80) for oxygen and 1.0×10^{17} cm^{-2} (ASTM F123-81) for carbon, and the carrier concentrations of the samples were determined from Hall-effect measurements at room temperature.

D. X-ray measurement

In the x-ray measurement the samples were mounted on a holder such that the rotation axis of the diffractometer was parallel to the [011] axis. With this orientation the reflections (200), (400), $(3\bar{1}\bar{1})$, $(4\bar{2}\bar{2})$, $(5\bar{1}\bar{1})$, etc., can be investigated. In these reflections we selected the larger and similar $\boldsymbol{h}$ pair, the (400) and $(3\bar{1}\bar{1})$ reflections. The (400) reflection was investigated in the symmetrical Bragg case and the $(3\bar{1}\bar{1})$ reflection was in the asymmetrical case. By measuring the Huang scattering near the (400) reflection in the perpendicular $\boldsymbol{q}$ direction, the parameter $\pi^{(3)}$ was determined (see Table I). The parameter $\pi^{(2)}$ was calculated from the scattered intensity in the perpendicular $\boldsymbol{q}$ direction at the $(3\bar{1}\bar{1})$ reflection, and then the parameter $\pi^{(1)}$ was calculated from that in the radial $\boldsymbol{q}$ direction at the (400) reflection. The lattice parameter was measured by a technique using two lattice planes mentioned above and monochromatic x-ray beams.[49,50] The accuracy of the lattice parameter measurement was $\pm 1 \times 10^{-4}$ Å.

IV. RESULTS

The results of diffuse x-ray intensity measurements for the Fz Si and thermally annealed Cz-Si crystals are shown in Fig. 2. Figures 2(a) and 2(b) are the intensities close to the (400) reflection measured in a direction parallel and perpendicular to the reciprocal lattice vector, respectively, and Fig. 2(c) is the intensity close to the $(3\bar{1}\bar{1})$ reflection in the perpendicular direction.

The asymmetry of the intensity pattern relative to the Bragg peak, that is, a stronger intensity at the right-hand side (positive $\boldsymbol{q}$) than the left one, is observed in Fig. 2(a). It means that the scattering is caused predominantly by a defect which produces a positive displacement of its neighboring atoms (an interstitial-type defect) and that the lattice parameter changes are positive.[43] This is in agreement with the result of the measurement of the lattice parameter change ($\Delta a/a = +2.7 \times 10^{-5}$). Furthermore, in Figs. 2(b) and 2(c), symmetric diffuse intensities are observed. Thus, additional weak diffuse intensities are observed in any direction for the annealed Cz Si crystal in comparison with the Fz Si reference crystal. Taking into account the low dislocation density in the annealed Cz Si crystal, it may be recognized that the extra diffuse scattering in the annealed Cz Si specimen is due to microdefects with a low-volume dilatation.

The Huang scattering intensity I_{Huang} is a symmetric part of the scattering intensity and is obtained by $I_{\text{Huang}} = \frac{1}{2}[I(\boldsymbol{q}) + I(-\boldsymbol{q}) - I_0(\boldsymbol{q}) - I_0(-\boldsymbol{q})]$, where I is the measured intensities and I_0 is the background. Figure 3 shows I_{Huang} near the (400) reflection parallel to the reciprocal lattice vector plotted in a semilogarithmic scale against q. Because of the no slit measurement in front of the counter (see Fig. 1), experimental data points in Fig. 3 show the characteristic feature as is expected in Eq. (9).[45] Hence it is possible to suppose that the predominant microdefects in the annealed Cz Si specimen are clusters being extrinsic in nature.

According to Eq. (9), if $q_0 = q_d \exp(0.5)$, the diffuse x-ray intensity becomes zero. This fact leads to a determination of the defect cluster size:

$$R_0 = \exp(0.5)[q_0(0)]^{-1}. \tag{12}$$

Here $q_0(0)$ is the intercept point of the linear portion with the abscissa axis as shown in Fig. 3. The cluster size, ~ 10 Å, is obtained directly from Eq. (12).

According to Table I and Eq. (3) the diffuse x-ray intensity measurement in the $\boldsymbol{q}$ direction [011] at the (400) reflection immediately gives the magnitude of $\pi^{(3)}$. From the value of $\pi^{(3)}$ and the measurement in the $\boldsymbol{q}$ direction [011] at the $(3\bar{1}\bar{1})$ reflection we get $\pi^{(2)}$, and from these $\pi^{(2)}$ and $\pi^{(3)}$ values and the measurement in the $\boldsymbol{q}$ direction [100] at
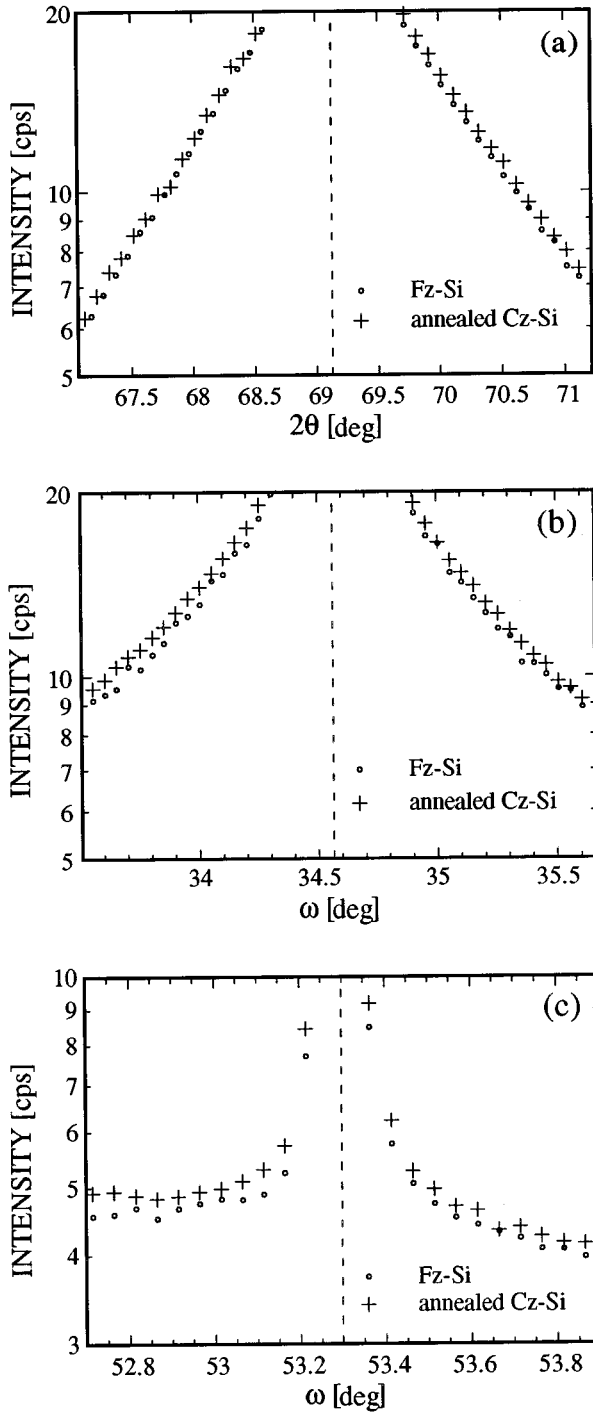
FIG. 2. Angular distribution of x-ray scattering intensities. (a) Near the (400) reflection in $\mathbf{q}$ direction $[100]$, (b) near the (400) reflection in $\mathbf{q}$ direction $[011]$, and (c) near the $(3\bar{1}\bar{1})$ reflection in $\mathbf{q}$ direction $[011]$.

FIG. 3. Dependence of the diffuse x-ray intensity on the deviation from the reciprocal lattice point. The error bars correspond to a confidence level of 90%.

the (400) reflection we get $\pi^{(1)}$. The value of $\pi^{(3)}$ is small and the $\pi^{(2)}$ is 3 times larger than the $\pi^{(3)}$ (see Table III). Therefore we can determine that the clusters in the annealed Cz Si have an orthorhombic symmetry ($\langle 110 \rangle$ defects). For a comparison of these symmetry parameters $\pi^{(2)}$ and $\pi^{(3)}$ with the theoretical predictions calculated from the thermal donor models, they were normalized by $\pi^{(1)}$, which is independent of the absolute defect strength. The experimental values are compared to those calculated theoretically from

the distortion results[30,36,51] around the thermal donor models as shown in Table III. In these calculations of the dipole force tensor, it is assumed that the displacements of the atoms far from the third-nearest neighbors are negligibly small, and we have used the isotropic approximation. In Table III, $(O_X)_n$ are the interstitial oxygen complexes, VO_n the oxygen + vacancy complexes, OBS and NL8 the oxygen + semivacancy complexes, and IO_2 the oxygen + self-interstitial complex, respectively. TD_3 and TD_4 are dominant thermal donors in a specimen annealed for 24 h at 450 °C,[22] and their symmetry parameters $\pi^{(2)}/\pi^{(1)}$ and $\pi^{(3)}/\pi^{(1)}$ are calculated from the total dipole force tensor which is added the dipole force tensor of two or three bond-centered interstitial oxygen atoms to that of the above defined core structure models. The experimental values should be compared to these two columns' values. The tendency of each complex type is the following: (a) Oxygen only, $\pi^{(3)}$ is extremely larger than $\pi^{(2)}$ or $\pi^{(2)}$ is zero within the error bar. It means a strong anisotropy and a small dilatation, and then all models are ruled out. (b) VO_n, in a small number of n (~ 2), $\pi^{(1)}$ is extremely small due to the cancellation of the volume dilatations from oxygens and the contraction to the vacancy; then $\pi^{(2)}$ and $\pi^{(3)}$ become large, and also ruled out. In VO_4^{2+} $\pi^{(2)}$ is zero, and then it is ruled out. (c) OBS, $\pi^{(2)}$ is very small or zero within the error bar, and then ruled out. NL8, $\pi^{(2)}$ is larger than $\pi^{(3)}$, which is due to the double force of the strength with P_{33} in the direction $\langle 001 \rangle$ is stronger than P_{11} in $\langle 110 \rangle$; then they are close to the experimental values. (d) IO_2, the tendency is the same with NL8. In addition to these results of the symmetry parameters of TD complexes, we have calculated those parameters for another $(O_i)_3$ core model[52] and the NO_2 one[53] proposed recently, and then their tendencies are similar to NL8 and IO_2 except for the more extremely strong force in the direction $\langle 001 \rangle$; it means that $\pi^{(2)}$ is larger than $\pi^{(3)}$ and they are also ruled out.

TABLE III. Experimental and theoretical values of the parameters $\pi^{(2)}/\pi^{(1)}$ and $\pi^{(3)}/\pi^{(1)}$ describing the deviation of the displacement field of cluster defects in annealed Cz Si from cubic symmetry. For complicated structures refer to Refs. 30, 36, and 51, and abbreviations to Sec. I. (-) indicates an extremely large value.

	Experimental values		Theoretical values for oxygen-related thermal donor models						
			(O_Y)	$(O_i)_2$	$(O_r)_2$	$(O_Y)_2$	O_2	$(O_i)_3$-1	$(O_i)_3$-2
$\pi^{(2)}/\pi^{(1)}$	0.065	core(TD$_1$)	0.616	0.000	0.290	1.039	0.775	-	0.0 17
		TD$_3$	0.022	0.000	0.058	3.635	6.822	0.032	0.005
		TD$_4$	0.011	0.000	0.035	11.396	-	0.014	0.003
$\pi^{(3)}/\pi^{(1)}$	0.017	core(TD$_1$)	0.112	0.148	0.080	1.013	1.560	-	0.8 97
		TD$_3$	0.199	0.000	0.135	5.256	9-24	0.441	0.065
		TD$_4$	0.243	0.019	0.171	29.738	-	0.409	0.045

		Theoretical values for oxygen-related thermal donor models							
		VO^0	VO^-	VO_2^0	VO_2^{2+}	VO_4^0	VO_4^{2+}	OBS	NL 8	IO_2
$\pi^{(2)}/\pi^{(1)}$	core(TD$_1$)	0.749	0.608	0.481	0.756	0.131	0.000	0.002	0.086	0.063
	TD$_3$	2.620	2.285	2.799	3.367	0.042	0.000	0.001	0.049	0.028
	TD$_4$	8.215	8.104	32.437	17.005	0.028	0.000	0.001	0.039	0.020
$\pi^{(3)}/\pi^{(1)}$	core(TD$_1$)	0.002	0.003	0.000	0.000	0.000	0.002	0.012	0.111	0.187
	TD$_3$	0.106	0.304	0.443	0.274	0.042	0.076	0.001	0.019	0.017
	TD$_4$	1.147	2.118	14.127	3.804	0.078	0.120	0.013	0.010	0.011

Therefore, we can select three core models VO_4^0, NL8, and IO_2, which are in agreement with the experimental values in the point of the same order of magnitude. However, because the measurements have been done at room temperature, it cannot be assumed that the donor states are neutral. Therefore the values observed for $\pi^{(2)}/\pi^{(1)}$ and $\pi^{(3)}/\pi^{(1)}$ seem to favor the models NL8 and IO_2 reasonably.

We finally evaluate the absolute concentration of defects, c, in Eq. (3). From the lattice parameter measurements performed in the Cz Si before and after annealing at 450 °C for 24 h under the same conditions we get $\Delta a/a = 2.7 \times 10^{-5}$. Combining this value with Eq. (5) we arrive at $c = 3.2 \times 10^{-6}$, that is, $1.6 \times 10^{17}/\text{cm}^3$ in Si crystal. In the other electrical measurement, the Hall-effect measurement has been performed for the carrier concentration in the annealed Cz Si specimen. Taking into account that the holes initially exist and that the TD is double donors, the evaluated donor concentration is $9 \times 10^{16}/\text{cm}^3$, which is generally in agreement with the diffuse x-ray scattering experiments. Some overestimation of the TD concentration by the diffuse scattering seems to be due to the presence of inactive complexes in the specimen. After annealing at 450 °C for 24 h the interstitial oxygen concentration calculated from the 9 μm absorption band of the FTIR region has been reduced to $5.8 \times 10^{17}/\text{cm}^3$, while the substitutional carbon concentration is unchanged. Then the number of oxygen atoms in a cluster defect can be determined from the reduction of the interstitial oxygen concentration and the creation of the defect concentration. On the average, a single-cluster defect contains seven oxygen atoms. This number is in good agreement with that of oxygen atoms in a thermal donor obtained experimentally by other authors.[14,21,23,38,54] Therefore, we have concluded that the main contribution to diffuse x-ray scattering intensities seem to be TD complexes.[55]

The estimated errors of the parameters $\pi^{(2)}/\pi^{(1)}$ and $\pi^{(3)}/\pi^{(1)}$ are $\pm 30\%$ and that of the c value from the x-ray measurement is $\pm 25\%$. Besides the statistical errors of the diffuse intensity measurements ($\pm 3\%$), they arise from the constants given in Table II, the error of the lattice parameter change ($\pm 11\%$ for $\Delta a/a$), and the possible inhomogeneity of the heat treatments of the samples. The errors of the concentrations from FTIR and the Hall-effect measurements are about $\pm 20\%$ and $\pm 10\%$, respectively.

V. SUMMARY

The diffuse x-ray scattering technique has been applied to investigate the thermal donor (TD) complexes in the Cz Si specimen annealed for 24 h at 450 °C. The measurements were made near the (400) Bragg reflection in the parallel direction to the reciprocal lattice vector and near the (400) and $(3\bar{1}1)$ in the perpendicular directions. The results indicate that the TD complexes are interstitial-type defect clusters and have an orthorhombic symmetry. The comparison between the symmetry parameters $\pi^{(2)}/\pi^{(1)}$ and $\pi^{(3)}/\pi^{(1)}$ obtained experimentally and those calculated theoretically from distorted atoms around the thermal donor models can be reduced to two reasonable models NL8 and IO_2 (self-interstitial and two oxygen atoms). Since NL8 and IO_2 core models are compatible with our results within the range of experimental errors, further experimental information is necessary to distinguish these two models.

[1] P. Ehrhart and W. Schilling, Phys. Rev. B **8**, 2604 (1973).

[2] P. Ehrhart and U. Schlagheck, J. Phys. F **4**, 1575 (1974).

[3] P. Ehrhart, H. D. Carstanjen, A. M. Fattah, and J. B. Roberto, Philos. Mag. A **40**, 843 (1979).

[4] R. S. Averback and P. Ehrhart, J. Phys. F **14**, 1347 (1984).

[5] U. Schubert, H. Metzger, and J. Peisl, J. Phys. F **14**, 2457 (1984).

[6] B. C. Larson and W. G. Schmatz, Phys. Rev. B **10**, 2307 (1974).

[7] I. Hashimoto and T. Yamazaki, Phys. Status Solidi A **147**, 45 (1995).

[8] A. N. Morozov and V. T. Bublik, J. Cryst. Growth **97**, 475 (1989).

[9] L. A. Charniy and V. T. Bublik, J. Cryst. Growth **135**, 302 (1994).

[10] C. S. Fuller, J. A. Ditzenberger, N. B. Hannay, and E. Buehler, Phys. Rev. **96**, 833 (1954).

[11] A. Bourret, in *Proceedings of the 13th International Conference on Defects in Semiconductors*, edited by L. C. Kimerling and J. M. Parsey, Jr. (Metal Society of AIME, New York, 1985), p. 129.

[12] P. Wagner and J. Hage, J. Appl. Phys. A **49**, 123 (1989).

[13] R. C. Newman, in *Proceedings of the 20th International Conference on the Physics of Semiconductors*, edited by E. M. Anastassakis and J. D. Joannopoulos (World Scientific, Singapore, 1990), p. 525.

[14] D. Wruck and P. Gaworzewski, Phys. Status Solidi A **56**, 557 (1979).

[15] H. F. Schaake, S. C. Barber, and R. F. Pinizotto, in *Semiconductor Silicon 1981*, edited by H. R. Ruff, R. J. Kriegler, and Y. Takeishi (Electrochemical Society, Pennington, NJ, 1981).

[16] R. Öder and P. Wagner, in *Defects in Semiconductors II*, edited by S. Mahajan and J. W. Corbett, MRS Symposia Proceedings No. 14 (North-Holland, New York, 1983), p. 171.

[17] M. Suezawa and K. Sumino, Mater. Lett. **2**, 85 (1983).

[18] B. Pajot, H. Compain, J. Lerouille, and B. Clerjaud, Physica B & C **117-118B**, 110 (1983).

[19] A. G. Steele and M. L. W. Thewalt, Can. J. Phys. **67**, 268 (1989).

[20] W. Kaiser, Phys. Rev. **105**, 1751 (1957).

[21] W. Kaiser, H. L. Firsch, and H. Reiss, Phys. Rev. **112**, 1546 (1958).

[22] A. Ourmazd, A. Bourret, and W. Schröter, J. Appl. Phys. **56**, 1670 (1984).

[23] A. R. Bean and R. C. Newman, J. Phys. Chem. Solids **33**, 255 (1972).

[24] S. Muller, M. Sprenger, E. G. Sieverts, and C. A. J. Ammerlaan, Solid State Commun. **25**, 987 (1978).

[25] K. M. Lee, J. M. Trombetta, and G. D. Watkins, in *Microscopic Identification of Electronic Defects in Semiconductors*, edited by N. M. Johnson, S. G. Bishop, and G. D. Watkins, MRS Symposia Proceedings No. 46 (Materials Research Society, Pittsburgh, 1985), p. 263.

[26] J. Michel, J. R. Niklas, and J.-M. Spaeth, Phys. Rev. Lett. **57**, 611 (1986).

[27] P. Wagner, H. Gottschalk, J. M. Trombetta, and G. D. Watkins, J. Appl. Phys. **61**, 346 (1987).

[28] M. Stavola and K. M. Lee, in *Oxygen Carbon, Hydrogen and Nitrogen in Silicon*, edited by J. C. Mikkelsen, Jr., S. J. Pearton, J. W. Corbett, and S. J. Pennycook, MRS Symposia Proceedings No. 59 (Materials Research Society, Pittsburgh, 1986), p. 95.

[29] J. L. Benton, L. C. Kimerling, and M. Stavola, Physica B & C **116B**, 271 (1983).

[30] P. Deák, L. C. Snyder, and J. W. Corbett, Phys. Rev. B **45**, 11 612 (1992).

[31] L. C. Snyder, J. W. Corbett, P. Deák, and R. Z. Wu, in *Defects in Electronic Materials*, edited by M. Stavola, S. J. Pearton, and G. Davies, MRS Symposia Proceedings No. 104 (Materials Research Society, Pittsburgh, 1988), p. 179.

[32] J. W. Corbett, R. S. McDonald, and G. D. Watkins, J. Phys. Chem. Solids **25**, 873 (1964).

[33] D. R. Bosomworth, W. Hayes, A. R. L. Spray, and G. D. Watkins, Proc. R. Soc. London, Ser. A **317**, 133 (1970).

[34] L. C. Snyder, P. Deák, R. Z. Wu, and J. W. Corbett, in *Proceedings of the 15th International Conference on Defects in Semiconductors*, edited by G. Ferenczi, Materials Science Forum Vols. 38–41 (Trans Tech Publications, Chur, Switzerland, 1989), p. 329.

[35] R. Jones, Semicond. Sci. Technol. **5**, 255 (1990).

[36] D. J. Chadi, Phys. Rev. B **41**, 10 595 (1990).

[37] M. Stavola and L. C. Snyder, in *Defects in Silicon*, edited by L. C. Kimerling and M. W. Bullis (Electrochemical Society, Pennington, NJ, 1983), p. 61.

[38] D. Helmreich and E. Sirtl, in *Semiconductor Silicon*, edited by H. R. Huff and E. Sirtl (Electrochemical Society, Pennington, NJ, 1977), p. 626.

[39] W. W. Keller, J. Appl. Phys. **55**, 3471 (1984).

[40] J. W. Corbett, J. Corelli, U. Desnica, and L. C. Snyder, in *Microscopic Identification of Electronic Defects in Semiconductors*, edited by N. M. Johnson, S. G. Bishop, and G. D. Watkins, MRS Symposia Proceedings No. 46 (Materials Research Society, Pittsburgh, 1985), p. 243.

[41] J. Michel, J. R. Niklas, and J.-M. Spaeth, Phys. Rev. B **40**, 1732 (1989).

[42] P. Deák, L. C. Snyder, and J. W. Corbett, Phys. Rev. Lett. **66**, 747 (1991).

[43] P. H. Dederichs, J. Phys. F **3**, 471 (1973).

[44] H. Trinkaus, Z. Angew. Phys. **31**, 229 (1971); Phys. Status Solidi B **51**, 307 (1972); **54**, 209 (1972).

[45] M. A. Krivoglaz, *X-Ray and Neutron Diffraction in Imperfect Crystals* (Naukova Dumka, Kiev, 1983).

[46] H. P. Klug and L. E. Alexander, *X-ray Diffraction Procedures for Polycrystalline and Amorphous Materials* (John Wiley & Sons, New York, 1954), p. 272.

[47] C. J. Sparks and B. Borie, *Local Atomic Arrangements Studied by X-Ray Diffraction*, Metallurgy Society Conference No. 36 (Gordon and Breach, New York, 1966).

[48] *International Tables for X-Ray Crystallography* (Kynoch, Birmingham, England, 1968).

[49] S. Kishino, Adv. X-Ray Anal. **16**, 367 (1973).

[50] S. Isomae, S. Kishino, K. Mukhopadhyay, and E. A. Starke, Jr., J. Appl. Crystallogr. **9**, 342 (1976).

[51] M. Saito and A. Oshiyama, Phys. Rev. B **38**, 10 711 (1988).

[52] D. J. Chadi, Phys. Rev. Lett. **77**, 861 (1996).

[53] C. P. Ewels, R. Jones, S. Öberg, J. Miro, and P. Deák, Phys. Rev. Lett. **77**, 865 (1996).

[54] D. K. Schroder, C. S. Chen, J. S. Kang, and X. D. Song, J. Appl. Phys. **63**, 136 (1988).

[55] J. J. Hall, Phys. Rev. **161**, 756 (1967).